Mon. Not. R. Astron. Soc. **000**, 000–000 (0000) Printed 5 February 2008 (MN LATEX style file v1.4)

Gravitational waves from newly born, hot neutron stars

V. Ferrari[1], G. Miniutti[1] and J.A. Pons[1,2]

[1] *Dipartimento di Fisica "G.Marconi", Università di Roma "La Sapienza" and Sezione INFN ROMA1, Piazzale Aldo Moro 2, I-00185 Roma, Italy*

[2] *Departament d'Astronomia i Astrofísica, Universitat de València, 46100 Burjassot, València, Spain*

5 February 2008

arXiv:astro-ph/0210581v2 2 Mar 2003

ABSTRACT

We study the gravitational radiation associated to the non–radial oscillations of newly born, hot neutron stars. The frequencies and damping times of the relevant quasi–normal modes are computed for two different models of proto–neutron stars, at different times of evolution, from its birth until it settles down as a cold neutron star. We find that the oscillation properties of proto–neutron stars are remarkably different from those of their cold, old descendants and that this affects the characteristic features of the gravitational signal emitted during the post-collapse evolution. The consequences on the observability of these signals by resonant–mass and interferometric detectors are analyzed. We find that gravitational waves from the pulsations of a newborn proto–neutron star in the galaxy could be detected with a signal to noise ratio of 5 by the first generation interferometers, if the energy stored in the modes is greater than $\sim 10^{-8}\ M_\odot c^2$, or by a resonant antenna if it is greater than $\sim 10^{-4}\ M_\odot c^2$. In addition since at early times the frequency of the spacetime modes is much lower than that of a cold neutron star, they would be also detectable with the same signal to noise ratio if a comparable amount of energy is radiated into these modes.

Key words: gravitational waves — stars: oscillations — stars:neutron

1 INTRODUCTION

According to the standard theory of star formation, neutron stars are born in the aftermath of successful core–collapse supernova explosions, as the stellar remnant becomes gravitationally

© 0000 RAS

decoupled from the expanding ejecta. Following the gravitational collapse, the proto–neutron star (PNS) radiates its binding energy (about 0.1 $M_\odot$) via neutrino emission in a timescale of tens of seconds. A small fraction of this energy reservoir is radiated in gravitational waves (GWs), and it is interesting to establish for how long, and at which frequencies the gravitational radiation will be emitted. The best currently available 2D-numerical simulations of a core collapse, and the most reliable estimates of gravitational wave emission consider, at best, the first hundred milliseconds from the collapse onset. In a number of axisymmetric simulations (Zwerger & Müller 1997; Dimmelmeier, Font & Müller 2002; Freyer, Holz & Hughes 2002), the flux of gravitational waves is evaluated through the quadrupole formalism, by using the time variation of the energy density of the collapsing system obtained either with Newtonian or general relativistic hydrodynamical codes. The emitted energy is estimated to range between 10^{-8} and $10^{-6} M_\odot$. Full three dimensional simulations in general relativity are not yet available, but there are some Newtonian studies (Rampp, Müller & Ruffert 1998; Brown 2001) that, by assuming small deviations with respect to axial symmetry, show similar results. In any event, the compact object which forms after the collapse possesses a certain amount of mechanical energy, which will partially be released through violent oscillations in the form of gravitational radiation.

The spectrum of the non–radial oscillations of a neutron star (NS) has a very rich structure that depends on how the temperature and the internal composition vary along its history. For instance, the frequency of the fundamental mode has been found to scale approximately as $\sim \sqrt{M/R^3}$, where M is the gravitational mass of the star and R is its radius, whereas that of the acoustic p–modes scales linearly with M/R. Since during the first tens of seconds of its life the star contracts and its gravitational mass decreases, one expects significant changes in the frequency of these modes. In addition, new families of modes may appear or disappear for several different reasons: *i)* as the star's entropy gradient decreases with time, the frequency of the gravity modes (g–modes) that are present at finite temperature migrate toward zero; *ii)* if no significant diffusion mechanism is present, layers of different chemical composition accumulating on the stellar surface would produce one or more density discontinuities, which would give rise to low frequency (typically < 200 Hz) discontinuity g–modes; *iii)* if the density of the inner core becomes high enough, a phase transition may occur, involving pion and/or kaon condensation as well as a transition from ordinary nuclear matter to quark matter (Prakash et al. and references therein 1997) which may produce a density discontinuity in the inner core of the star. In this case, a new discontinuity g–mode

would appear, at a frequency higher than the previous ones - typically > 700 Hz - (Sotani, Tominaga & Maeda 2002; Miniutti et al. 2002); *iv)* in previous works (Reisenegger & Goldreich 1992; Lai 1994) it has been shown that g-modes due to composition gradients in the inner core of cold NSs have typical frequency below 200 Hz. In hot PNS, the composition gradients are larger and produce g-modes of higher frequencies, even at constant entropy. *v)* Finally, it should be mentioned that relativistic stars do also possess a family of modes, called w–modes, that are associated to perturbations of the gravitational field, and couple very little (or do not couple at all, as for the axial w–modes) with the motion of the fluid (Chandrasekhar & Ferrari 1991; Kokkotas & Schutz 1992). The properties of the w–modes depend on the internal composition of the star (Andersson & Kokkotas 1996; Benhar, Berti & Ferrari 1999), and therefore they also change as the star evolves.

In this paper we study how the characteristic frequencies and damping times of some relevant classes of quasi–normal modes (QNMs) of a newly born, hot PNS change during its early evolution until it settles as a cold, catalyzed NS. Despite the fact that PNSs are expected to be born with a significant amount of angular momentum, in this work we neglect the effects of rotation. In this way, we can isolate and better understand the effects of the thermal and chemical evolution, and we can also clearly indicate the differences between hot PNS and cold NS oscillation properties. This study gives an interesting indication of the frequency range where the gravitational signals emitted immediately after gravitational collapse should be looked for. The paper is organized as follows. In Section 2 we review the evolutionary stages immediately following the birth of a proto–neutron star and discuss the dissipative precesses and timescales relevant during the Kelvin-Helmholtz epoch. In Section 3, we remind the physical processes that produce the gravity modes, and shortly describe the procedure we use to compute the QNM frequencies. The results of our study are presented in Section 4, where we also discuss the detectability of the gravitational signal associated to the quasi–normal modes by resonant bars or ground based interferometric detectors. The main findings of the paper are summarized in the concluding remarks.

2 THE FIRST MINUTE OF A NEUTRON STAR LIFE.

A newly born PNS is very different from its cold descendant, i.e. a NS. Indeed, initially, the PNS is hot, lepton rich, and optically thick to neutrinos, which are temporarily trapped within the star. The subsequent evolution is dominated by neutrino diffusion which first

deleptonizes and later cools the star (Burrows & Lattimer 1986). The evolution of a PNS proceeds through several distinct stages and has been recently studied in great detail, including the possibility of developing a core of exotic matter such as hyperons, a kaon condensate, or quark matter. The results we present in this paper are based on simulations of PNS evolution described in Pons et al. (1999; 2000; 2001). We consider two models of PNS evolution, that use two different equations of state (EOSs). In both cases the EOS of baryonic matter is a finite-temperature, field-theoretical model solved at the mean field level, where the interactions between baryons are mediated by the exchange of σ, ω and ρ mesons. Electrons and muons are included in the model as non interacting particles, being the contribution due to their interactions much smaller than that of the free Fermi gas. We consider two of the models of evolving PNS studied by Pons et al. (1999; 2001) where neutrino transport is treated using the diffusion approximation, that allows to obtain global properties of the neutrino emission, like average energies, integrated fluxes and timescales. Model A has a soft EOS (Glendenning & Moszkowski 1991) while model B is stiffer (Müller & Serot 1996) and allows for the formation of a quark core at some point of the evolution. The mixed phase of baryons and quarks is constructed to satisfy Gibbs' phase rules for mechanical, chemical and thermal equilibrium, assuming global charge neutrality. The quark matter EOS is computed using the MIT bag model (with Bag constant B= 150 MeV/fm^3). A detailed discussion on the EOS, on the evolution of PNSs and on the microphysical inputs (opacities) can be found in the above references. However, here it is useful to summarize the different stages of the early evolution of a PNS referring, as an illustrative example, to Model A. In Figure 1 we show some relevant physical variables that characterize the PNS status at different instants of time (0, 0.1, 1, 5, 10, 40 seconds): the entropy per baryon, s, the temperature T, the electron neutrino chemical potential μ_ν, and the radius R. Each quantity is plotted versus the enclosed baryonic mass, M_B.

The different stages of the early evolution can be summarized as follows.

i) Immediately after the core bounce and the passage of the shock wave through the outer PNS mantle, the star contains an unshocked, low entropy core of mass $\simeq 0.7$ M$_\odot$ in which neutrinos are trapped. The core is surrounded by a low density, high entropy mantle (see Figure 1, left–bottom) that is accreting matter falling through the shock from the outer iron shell and it is rapidly losing energy due to electron captures and thermal neutrino emission. The mantle extends up to the shock, which is temporarily stalled at a radius of about 200 km prior to an eventual explosion. If the supernova is successful, after a few hundred milliseconds

accretion becomes unimportant and the shock lifts off the stellar envelope. In a few tens of seconds, extensive neutrino losses reduce the lepton pressure provoking the contraction of the mantle. The radius of the PNS is now about $20 - 30$ km.

ii) Neutrino diffusion deleptonizes the core on a time scale of $10 - 15$ s. The diffusion of degenerate, high-energy (200 MeV) neutrinos from the core to the surface, from where they escape as low-energy neutrinos ($10 - 20$ MeV), generates a large amount of heat within the star, resulting in temperatures up to 50 MeV, while the core entropy approximately doubles (see Figure 1, left panels). The inverse temperature gradient which arises in the inner region produces a heat wave that propagates inward. At the end of the deleptonization epoch, the star reaches its maximum central temperature.

iii) After approximately 15 s, the PNS has become lepton-poor but it is still hot. The net number of neutrinos in its interior is low, but thermally produced neutrino pairs of all flavors are abundant and dominate the emission. Thus, neutrino diffusion continues to cool the star, while the average neutrino energy decreases, and the neutrino mean free path increases. After approximately 50 seconds, the mean free path becomes comparable to the stellar radius, and the star finally becomes transparent to neutrinos. By this time, the temperature has dropped to $1-5$ MeV ($\approx 10^{10}$ K) and the star has radiated almost all of its binding energy. A neutron star is born.

2.1 Dissipation time scales

Since the focus of this paper is on the emission of gravitational radiation produced by the violent pulsations of a newly born PNS, it is crucial to understand whether these oscillations may be damped by other dissipative processes acting on timescales shorter than the typical gravitational timescales.

We have seen that in a PNS the energy is transferred and redistributed dominantly by neutrino diffusion. Hence, when one considers hydrodynamical processes, the relevant dissipation time-scales are those corresponding to the neutrino viscosity, diffusivity, thermal conductivity, or thermodiffusion, rather than those associated to the matter kinetic coefficients. Transport properties of degenerate neutrinos in dense matter were studied in detail by Goodwin & Pethick (1982) and by van den Horn & van Weert (1984). They found that for the thermodynamical conditions typical in PNSs and for strongly degenerate neutrinos ($\mu_\nu \gg k_B T$) the dominant dissipative process is neutrino chemical diffusion, fol-

lowed by thermal conduction and viscosity. Thus, the hierarchy of dissipation timescales is $\tau_D < \tau_C < \tau_{visc}$, where τ_D, τ_C, and τ_{visc} are the diffusion, thermal conduction, and viscous timescales, respectively. τ_D can be estimated by the following approximate relations (van den Horn & van Weert 1984)

$$\tau_D(\mathrm{s}) \approx 24\ s\ n_B^{1/3} \left(\frac{0.01}{Y_\nu}\right) \left(\frac{T}{10\mathrm{MeV}}\right) \left(\frac{\mu_\nu}{100\mathrm{MeV}}\right), \tag{1}$$

where s is the entropy per baryon in units of the Boltzmann constant, n_B is the baryon density (in fm^{-3}), and Y_ν is the neutrino fraction.

Conversely, if neutrinos are non-degenerate ($\mu_\nu \ll k_B T$), the hierarchy between neutrino diffusion and thermal conduction is reversed and $\tau_C < \tau_D < \tau_{visc}$. In this case τ_C can be expressed as (van den Horn & van Weert 1984)

$$\tau_C(\mathrm{s}) \approx 1.5\ s\ n_B^{1/3} \left(\frac{0.01}{Y_\nu}\right) \left(\frac{T}{10\mathrm{MeV}}\right)^2, \tag{2}$$

In both cases, the timescale τ_{visc} is a factor $10 - 50$ longer.

In summary, during the first $10 - 20$ seconds of the star life, diffusion is the dominant dissipative process in the inner regions (where neutrinos are degenerate), while thermal conduction dominates in the outer region. Afterwards, thermal conduction becomes the more efficient mechanism of energy dissipation until the matter composing the star becomes transparent to neutrinos. The order of magnitude of both τ_D and τ_C varies from a few seconds to tens of seconds, and it is comparable to the overall evolutionary timescale. This is shown in Figure 2, where the diffusion (solid line) and the conductive (dashed line) timescales are plotted as a function of the radius for model A, and $t = 0.25$ seconds after the birth of the PNS. The dotted line is the degeneracy parameter of neutrinos ($\eta = \mu_\nu / T$), and it is shown to indicate in which region τ_D and τ_C dominate. As a rule of thumb, τ_D must be used when $\eta > 1$, while τ_C is the relevant timescale when $\eta < 1$. In conclusion, a conservative estimate of the dissipative timescales before neutrino transparency is $\tau_D \approx \tau_C \approx 10 - 20$ seconds. In the following we will denote by τ_{diss} the minimum of the typical dissipative timescales, $\tau_{diss} = \min(\tau_D, \tau_C, \tau_{visc})$.

3 QUASI-NORMAL MODES OF RELATIVISTIC STARS

In order to understand what are the differences between the oscillation properties of PNSs and those of old, cold NSs, we shall briefly recollect some results obtained in the literature for cold NSs. A systematic analysis of the pulsation properties of cold NSs has been done

by Andersson and Kokkotas (1998) for a large range of EOSs; they found a set of empirical relations that connect the mode frequencies and damping times to the mass and radius of the star. As an example, from their relations one finds that for a cold NS with $M = 1.4 M_{\odot}$ and $R = 10$ km the inferred values of the frequency and damping times of the f–mode, and of the first p– and w– modes for $l = 2$ are

$$\begin{aligned} \nu_f &\approx 2 \text{ kHz} , \qquad \nu_{p_1} \approx 7 \text{ kHz} , \qquad \nu_{w_1} \approx 11.8 \text{ kHz} , \\ \tau_f &\approx 10^{-1} \text{ s} , \qquad \tau_{p_1} \approx 5 \text{ s} , \qquad \tau_{w_1} \approx 2.4 \times 10^{-5} \text{ s} . \end{aligned} \tag{3}$$

A further family of modes which may appear in NSs are the so-called gravity or g–modes, whose restoring force is buoyancy. It is known (e.g. Thorne 1966) that the radial acceleration of a fluid element displaced by its equilibrium position can be written as

$$a = -\frac{e^{-\lambda/2}}{(\epsilon + p)\gamma p} \left(-\frac{dp}{dr} \right) S(r)\, \Delta r , \tag{4}$$

where ϵ and p are the energy density and the pressure, Δr is the radial displacement of the fluid element, $\gamma = [(\epsilon + p)/p][\partial p/\partial \epsilon]_{s,Y_L}$ is the adiabatic index, with Y_L being the lepton fraction, $-e^{\lambda}$ is the g_{rr} component of the unperturbed metric tensor, and

$$S(r) = \frac{dp}{dr} - \frac{\gamma p}{\epsilon + p} \frac{d\epsilon}{dr} \tag{5}$$

is the relativistic Schwarzschild discriminant. If $S(r) > 0$, the displaced fluid element feels a force that tends to restore the initial equilibrium position and the star (or the region inside the star) is stable against convection. In this case, a non–zero frequency spectrum of stable g–modes appear. Conversely, if $S(r) < 0$, the force tends to move the fluid element away from equilibrium and the star becomes unstable against convection. Finally, if $S(r) = 0$, all g–modes are degenerate at zero frequency.

By introducing the adiabatic sound velocity, c_s^2, which is defined at constant entropy s and chemical composition, and the so–called equilibrium velocity, c_0^2,

$$c_s^2 = \left(\frac{\partial p}{\partial \epsilon} \right)_{\mathrm{s,Y_L}} = \frac{p}{\epsilon + p}\, \gamma , \qquad c_0^2 = \frac{dp/dr}{d\epsilon/dr} , \tag{6}$$

the Schwarzschild discriminant (5) can be cast into a form which will be useful in following discussions

$$S(r) = \frac{dp}{dr} \left(1 - \frac{c_s^2}{c_0^2} \right) . \tag{7}$$

Thus, a stable g–mode arises only if $c_s^2 > c_0^2$, and the buoyancy which provides the restoring force can be induced either by entropy and/or composition gradients (McDermott, van Horn & Hansen 1988; Reisenegger & Goldreich 1992; Lai 1994), by density discontinuities in the

outer envelopes of NSs (Finn 1987; Strohmayer 1993), or by density discontinuities in the inner core as a consequence of phase transitions at high density (Sotani, Tominaga & Maeda 2002; Miniutti et al. 2002). The frequency of the g–modes is always lower than that of the f–mode, it is roughly proportional to the Schwarzschild discriminant, and depends on the physical process which is source of the buoyancy. In general, the g–modes of cold NSs have a typical frequency of less than 200-300 Hz and very long damping times (typically, $\tau_g > 10^6$ s). We shall see that the situation is different during the first second of life of a PNS.

3.1 Computation of the modes

In this subsection we clarify some technical aspects of the computational procedure we use to find the frequencies and damping times of the quasi–normal modes. We integrate the equations describing the polar, non radial perturbations of a non rotating star in general relativity. We use the same formulation of the perturbed equations as in Miniutti et al. (2002), based on the work of Detweiler & Lindblom (1985), who derived a fourth order system of equations for the metric and fluid perturbations inside the star. However, we do not use their original method, because we integrate the system in the complex frequency domain directly, rather than working in the real frequency domain. The system of perturbed equations is closed by the equation of state. In particular, the equilibrium profiles of the energy density and of the sound velocity are sufficient to completely solve the perturbation equations in the stellar interior. The profiles we use are the same as those obtained in Pons et al. (1999; 2001).

The set of equations, that couple the perturbations of the fluid with those of the gravitational field, are Fourier expanded and separated by expanding the perturbed tensors in tensorial spherical harmonics. For each assigned value of the harmonic index l and of the (complex) frequency ν , the system of equations admits only two linearly independent solutions regular at $r = 0$. The general solution can be found as a linear combination of the two, such that the Lagrangian perturbation of the pressure, Δp , vanishes at the surface. Outside the star, the fluid perturbations vanish and the system reduces to the Zerilli equation (Zerilli 1970). A quasi normal mode of the star is defined to be a solution of the perturbed equations belonging to a complex eigenfrequency, which is regular at the center, continuous at the surface, and which behaves as a pure outgoing wave at infinity. To compute the QNM complex eigenfrequencies we follow the method developed by Leins, Nollert

and Soffel (1993) who derived a procedure (the continued fractions method) to evaluate a function which is proportional to the ingoing part of the wave, and therefore vanishes when ν is an eigenfrequency of a QNM. A very clear account of the method can be found in Sotani, Tominaga & Maeda (2002).

4 THE GRAVITATIONAL WAVE SPECTRUM OF A PROTO-NEUTRON STAR.

Using the method described in Section 3, we have computed the quasi–normal mode frequencies and damping times of the two models of proto–neutron star, at different instant of time from $t = 0.2$ s to $t = 50$ s after their formation. The configurations we consider as initial refers to $t = 0.2$ s for both models, because at earlier times the PNS evolution could be affected by dynamical processes like accretion, and cannot be accurately approximated by a quasi–stationary series of solutions of the hydrostatic equations. Thus we exclude from our study the collapse, the bounce and the first two hundred milliseconds after formation, for which more detailed hydrodynamical simulations are needed.

At $t = 0.2$ s, model A has $M = 1.58\ M_\odot$ and $R = 34.2$ km, while model B has the same mass and $R = 35.1$ km. Both models are chosen such that the final stage of the PNS evolution, at $t = 50$ s in our simulations, represents a "canonical" NS with a mass of about $M = 1.46 M_\odot$ and a radius of $R \sim 12 - 13$ km. The gravitational mass difference between the initial and final configurations ($\approx 0.12 M_\odot$) has been taken away by neutrinos during the PNS evolution. In the following, we shall discuss the behavior of the frequencies of the fundamental mode, and the first g–, p– and w–modes for $l = 2$, as the star evolves and cools down. To identify the different classes of fluid modes we study the behavior of the Lagrangian radial displacement. The eigenfunction of the f–mode has no radial nodes, while the g_1– and p_1–modes have one radial node. The w_1–mode is easily identified, because it produces negligible motion in the fluid, and because its damping time is much shorter than that of the fluid modes.

The QNM frequencies and damping times for model A and B are tabulated in Tables 1 and 2 at different values of the evolution time. The oscillation properties within the first 5 seconds of the PNS evolution are summarized in Figure 3 for both models.

We find that during the first seconds of life of the PNS the frequencies of the f–, p_1– and w_1– modes are much lower than those of the cold neutron star which results at the end

of the evolution. Initially, they cluster in a narrow range within $[900 - 1500]$ Hz, and if we compare the value that a given mode frequency has at $t = 0.2$ s and at $t = 50$ s, we find a difference of about 40% for the f–mode, $\sim 75\%$ for the p_1–mode and of $\sim 65\%$ for the w_1–mode. This significant difference can be attributed partly to the fact that at earlier times the PNS is less compact, and partly to the very reach thermodynamical structure that characterizes the first few seconds of the PNS life (see Figure 1). In this respect, the behavior of the the f–mode frequency is of particular interest, since it does not scale with $\sqrt{M/R^3}$ as it does for cold NSs: indeed, Tables 1 and 2 show that, during the first second, the mass of the star remains approximately constant while the radius rapidly decreases, and consequently ν_f should increase; on the contrary, it initially decreases, at about $t \approx 0.5$ s approaches the value of the g–mode frequency, and only after about one second, it starts to increase linearly with $\sqrt{M/R^3}$. At the same time, the g_1–mode frequency increases when the star is younger and hotter and large thermal and composition gradients dominate in the interior, it reaches a maximum value of about $800 - 900$ Hz within the first second of life, and afterwards, as the star cools down and entropy gradients are smeared out, it migrates towards lower values. Even though there is a point of the evolution when ν_f and ν_{g_1} are very close (see Figure 3), the two modes are always distinguishable because of the different number of nodes in their eigenfunctions.

From Tables 1 and 2, we see that after a few seconds from birth, the damping times of the f, p_1 and w_1–modes of the PNS are quite close to those of its cold descendant. At very early times ($0.2 < t < 2$ s) the situation is different; for instance, τ_f decreases rapidly from ~ 70 s to $\sim 2 - 3$ s, and it is interesting to compare its values with τ_{diss}, which is about 10-20 seconds, as explained in Section 2.1. For $t \lesssim 0.5$ seconds, $\tau_{diss} < \tau_f$, therefore during this time, a small fraction of the amount of energy initially stored in the f–mode, will be dissipated by neutrino processes. However, for $t \gtrsim 0.5$ seconds, τ_f becomes smaller than τ_{diss}, and gravitational wave emission becomes the dominant dissipation mechanism. In addition, apart from the first few tens of milliseconds, the p_1–mode damping time is always comparable to τ_{diss}, while τ_{w_1} is basically unaffected by the evolution and it is by far the shortest one. Therefore, if some energy is initially stored into these modes, it will be emitted in gravitational waves.

Furthermore, we find that during the first second, the g_1–mode damping time is much shorter than that expected from previous calculations for cold NSs. In particular, for both PNS models τ_{g_1} is comparable to τ_f, to τ_{p_1} and also to the neutrino dissipation timescale

during the first half a second. Thus, the common belief, based on cold NSs dynamical behavior, that the damping time of the f–mode is an order of magnitude shorter than that of the first p–mode and many orders of magnitude smaller than the g–modes damping times, is no longer correct during the first second of life, which is likely to be the most important for the emission of GWs.

For g–modes of order higher than one, we find damping times much larger than that of the g_1–mode; For instance, the g_2–mode has a damping time of the order of 10^4 s at $t = 0.4$ s. Thus, g–mode pulsations of order higher than 1 are unlikely to be significant sources of gravitational radiation and will be neglected in our analysis.

From Tables 1 and 2 we see that, for $t \gtrsim 10 - 20$ seconds, the g_1–mode frequency of both models increases. As explained in Section 3, g–modes can be associated to several physical processes, and during the early evolution of a PNS they arise mainly because there are large entropy and composition gradients. While during the deleptonization epoch entropy gradients dominate the dynamical behavior of the star, after some time composition gradients become important, and this change produces a modulation in the frequency of the g–modes. In addition, at $t = 50$ s we see that ν_{g_1} of model A and B are different. The reason can be understood by looking at Figure 4, where we plot c_s^2 and c_0^2 as a function of the radial distance at $t = 50$ s. For model A the difference between the two quantities is small compared to model B, which develops a quark core and an associated larger composition gradient. As discussed in Section 3, this explains why the frequency of the g_1–mode for model B is larger than that of model A.

Finally, it should be mentioned that the frequency of the first w–mode ranges within $[1.4 - 1.8]$ kHz, which is about one order of magnitude smaller than the typical value of a cold NS, while the damping time is similar, and very short ($\sim 10^{-4}$ s), much shorter than τ_{diss}.

4.1 Gravitational wave detectability

The fact that during the early evolution of a PNS the frequencies of the quasi–normal modes are much lower than those of the final NS is of particular interest, since the region where the interferometric antennas of first generation are more sensitive does not extend much beyond 1 kHz. This means that waves emitted at the frequencies of the QNMs of a cold NS will not be detectable (see Eqs. 3).

Unfortunately we do not know how the mechanical energy is distributed among the various modes, but we cannot exclude a priori that at very early times, besides the f–mode, the first g–mode or the first p–mode could give a contribution to the emitted wave, therefore we will consider each mode separately and we will proceed as follows. Having calculated how the frequencies and damping times evolve in time, we can model the gravitational signal emitted by the star oscillating in a given mode as

$$h(t) = h_0 \, \mathrm{e}^{-(t-t_0)/\tau(t)} \sin[\, 2\pi\nu(t)(t-t_0)\,] \, , \tag{8}$$

where h_0 is the initial amplitude at the detector site, t_0 is the arrival time, $\nu(t)$ is the frequency of the oscillation, and $\tau(t)$ is the gravitational damping time of the oscillation. The signal–to–noise ratio (SNR) of a given detector is evaluated by using the standard formula for optimal matched filtering

$$SNR = 2 \left[\int_0^\infty d\nu \, \frac{|\tilde{h}(\nu)|^2}{S_n(\nu)} \right]^{1/2} , \tag{9}$$

where $S_n(\nu)$ is the noise power spectral density of the detector. We shall use the noise curves of VIRGO I, LIGO I, GEO600 (Grishchuk et al. 2001, and references therein), and that of EURO (http://www.astro.cf.ac.uk/geo/euro/), an interferometric detector with extremely high sensitivity in the kHz region whose performances have been devised by a joint panel of European experts.

We discuss the results of our calculations for model B, but similar results are obtained for model A. Since the emission of gravitational waves is efficient only if the gravitational damping time $\tau(t)$ is comparable or shorter than the dissipative timescale τ_{diss}, the gravitational signal produced by the various modes has been considered different from zero only if the condition $\tau(t) \lesssim \tau_{diss}$ is satisfied.

In Table 3 we show the values of the initial amplitude h_0 that a given signal with the form (8) should have to be detectable with a SNR=5. In addition, we can estimate the amount of energy emitted by a source by integrating over the frequency and the surface the expression of the energy flux

$$\frac{dE_{\rm GW}}{dSd\nu} = \frac{\pi}{2} \, \nu^2 \, |\, \tilde{h}(\nu) \, |^2, \tag{10}$$

In Table 3 we also give the energy E_{GW} that should be emitted by a galactic source oscillating in a given mode to reach SNR=5. Notice that, since the energy scales as D^2, the energy required to detect the same signal emitted by a source in the Virgo cluster (15 Mpc) with SNR=5 is simply given by $2.25 \times 10^6 E_{GW}$.

From Table 3, we see that a signal detectable by the first generation of ground–based interferometers with SNR=5 must have an initial amplitude larger than 10^{-22}. For instance, $h_0 = 2.3 \cdot 10^{-22}$ for VIRGO I, if emitted by an f–mode oscillation. This amplitude corresponds to an emission of energy of $3.5 \times 10^{-8}\ M_\odot c^2$, in the event of a galactic Supernova. This is consistent with recent studies of the axisymmetric collapse of the core of a massive star, where the energy emitted in gravitational waves, averaged over all the considered models, is estimated to range within $[3.6 \cdot 10^{-8} - 8.2 \cdot 10^{-8}]\ M_\odot c^2$ (Dimmelmeier, Font & Müller 2002). In the above reference, the corresponding average amplitude for a source at 10 kpc is about 1.7×10^{-20}, and the average spectrum of gravitational emission is peaked at 930 Hz.

The advanced interferometer EURO would be able to detect signals with initial amplitude $h_0 \gtrsim 8 \cdot 10^{-25}$ with SNR=5 (see Table 3). For sources located at the distance of the Virgo cluster this corresponds to an emission energy of the order of $10^{-8}\ M_\odot c^2$, with a multiplicative factor depending on the particular fluid mode. Thus, a detector like EURO would increase the detection rate for Supernova events from a few events per century to a few events per month.

The role of the spacetime w_1–mode deserves a separate discussion. It is interesting to note that for the w–modes the amount of energy required for the GW to be detected is similar to that of fluid modes (see Table 3) despite the wave amplitude has to be larger. This is essentially due to the smaller gravitational damping time, $\tau_{w_1} \sim 10^{-4}$ s. However, these modes are very weakly coupled to the fluid, and it remains unclear whether this small amount of energy can be effectively conveyed into spacetime oscillations.

We have also analyzed the response of a resonant mass detector to the gravitational signals computed in this paper. In Figure 5 we plot the experimental noise strain amplitude of EXPLORER obtained in December 2001 (http://www.roma1.infn.it/rog/explorer/), the strain noise curve that the EXPLORER team expects to obtain in 2003 reducing the noise and increasing the quality factor (Astone 2002), and the strain amplitude produced by the f– and g_1–mode, corresponding to a SNR= 5. From the figure we see that only the f–mode signal falls in the region of best sensitivity. By using the 2003 noise curve, we find that it would be detected with SNR= 5 if the amplitude on Earth is $h_0 \simeq 3 \cdot 10^{-20}$, i.e. $E_{GW} \simeq 6 \cdot 10^{-4}\ M_\odot c^2$ for a galactic source. However, this is only an indication; indeed, rotation or different details of the dynamical evolution of the star may shift the two contributions in a way that either the g–modes, or both modes may fall inside the sensitivity band. In addition, better sensitivities will be reached in the next future by the bars further refining the experimental setting. With

the expected improvements (M. Bassan, private communication) we find that E_{GW} can be lowered by at least an order of magnitude.

5 CONCLUDING REMARKS

In this paper we show that the frequency and the damping time of the QNMs of a newborn proto–neutron star change significantly as the star cools down and deleptonizes. In particular, at early times, when most of the gravitational energy is emitted, the typical frequencies are considerably lower than those of cold NSs. In order to understand whether the dissipative processes acting in a young PNS could damp the oscillations of the star more efficiently than gravitational waves, we have compared the gravitational damping times to the timescales associated to neutrino viscosity, diffusivity and thermal conductivity ($\tau_{diss} \approx 10 - 20$ s). We find that, during the first half a second, neutrino processes dominate with respect to the gravitational emission due to the f–mode. However, this time interval is very short compared to τ_{diss}, and therefore no much of the energy initially stored into the mode will be dissipated by neutrino diffusion. After half a second, the gravitational damping time of the f–mode becomes shorter than τ_{diss} and, consequently, the remaining mechanical energy can be freely released in gravitational waves. The p–mode damping time is always comparable to τ_{diss}, while the gravitational emission from g–modes could be expected only during the first half a second of the evolution, when the g–mode damping time is comparable to τ_{diss}. The w–mode damping time is always orders of magnitude smaller than τ_{diss}.

We have restricted our analysis to two models of PNS evolution, but we do not expect qualitative changes if different EOSs are used. For example, by changing the symmetry energy of the equation of state one can vary the final composition gradient. For changes in a physically reasonable range, the g_1–mode frequency of the final, cold neutron star may vary between 100-300 Hz for the model without a phase transition, and higher values would be reached if a phase transition to quark matter occurs. From our data (Tables 1 and 2) we see that during the first second of evolution ν_{g_1} varies within $\sim [600 - 800]$ Hz, ν_f within $\sim [900 - 1100]$ Hz, and ν_{g_1} reaches a maximum approximately when ν_f has a minimum; it is reasonable to expect that these features will not change significantly for different initial models.

As shown in Section 4.3, a gravitational signal, emitted at the frequency of the quasi–normal modes of a newborn proto–neutron star in the galaxy, could be detected with a signal

to noise ratio of 5 by the first generation interferometers if the energy stored in the modes is greater than $\sim 10^{-8}\ M_\odot c^2$ (or by a resonant antenna if it is greater than $\sim 10^{-4}\ M_\odot c^2$). It is interesting to stress that the f–, p– and w–modes have frequencies much lower than those of the cold neutron star which forms at the end of the evolution, in a region where the detectors sensitivity is higher and the energy threshold for detection is lower.

Unfortunately, a galactic Supernova is a very rare event (≈ 3 per century). However, there is another astrophysical scenario to which the results of our study could be applied. Recent numerical simulations (Shibata & Uryu 2000; Shibata & Uryu 2002) have shown that short-lived supra-massive neutron stars can also be formed following the merger of two neutron stars with nearly equal masses and low compactness. These highly non axisymmetric objects are supported by differential rotation and would emit quasi-periodic gravitational waves with typical frequencies of $\sim 2-3$ kHz. The results of these simulations show that up to 0.01 $M_\odot$ could be radiated in gravitational waves, as opposed to the 10^{-8}–$10^{-6}\ M_\odot$ usually obtained for stellar core collapse. In these works, the coalescing stars are assumed to have a polytropic EOS and thermal effects are not included, thus the peak frequency corresponds to the excitation of the f-mode frequency of a cold neutron star. The fastly rotating PNS born as a consequence of the coalescence of low compactness neutron stars, should have thermodynamical properties similar to those of the PNSs we study in this paper. Therefore, we think that the effects of thermal and composition gradients we have found should produce a similar shift in frequencies and damping times with respect to the cold star case, but with the remarkable difference that these metastable PNSs would be much stronger emitters of GWs. The large amount of emitted energy would make the ringing down of the PNS observable from the Virgo cluster, increasing the event rate to a few per year.

Acknowledgements

We thank P. Astone for kindly providing the experimental curves of the noise of EXPLORER and for interesting discussions.

This work has been supported by the EU Programme 'Improving the Human Research Potential and the Socio-Economic Knowledge Base' (Research Training Network Contract HPRN-CT-2000-00137) and the Spanish Ministerio de Ciencia y Tecnologia grant AYA 2001-3490-C02-01. JAP was supported by the Marie Curie Fellowship No. HPMF-CT-2001-01217.

Table 1. The frequencies (in Hz) and damping times (in s) of the first g–mode, the fundamental mode, the first p–mode, and the first w–mode are given for different values of time (in s) for the PNS evolution, model A. The damping time of the g_1–mode for $t > 3$ s is not shown because it is so long that the oscillation will be damped by neutrinos rather than by GWs. As a reference, we indicate also the radius (in km) of the PNS at each considered time step. The gravitational mass is $M = 1.58 M_\odot$ for our initial model at $t = 0.2$ s, and $M = 1.46 M_\odot$ at $t = 50$ s. The gravitational mass difference ($\approx 0.12 M_\odot$) has been taken away by neutrinos during the PNS evolution.

t	R	ν_{g_1}	τ_{g_1}	ν_f	τ_f	ν_{p_1}	τ_{p_1}	ν_{w_1}	$10^4 \times \tau_{w_1}$
0.20	34.2	617.1	21.8	953.1	60.2	1221.5	11.8	1597.5	2.00
0.25	31.2	677.0	17.4	948.9	38.6	1366.2	9.1	1781.7	1.92
0.30	28.9	727.0	15.2	943.8	27.1	1487.1	7.7	1943.3	1.87
0.40	25.7	796.4	16.9	941.6	12.6	1684.9	6.6	2213.5	1.78
0.50	23.7	819.9	35.8	960.9	7.1	1833.5	6.3	2413.0	1.73
0.60	22.3	815.4	100.6	994.4	5.4	1954.8	6.2	2573.4	1.69
0.70	21.3	799.5	270.8	1031.4	4.7	2057.6	6.3	2712.9	1.66
0.75	20.9	790.3	415.4	1048.5	4.4	2100.4	6.3	2772.9	1.65
1.0	19.4	744.1	2.4×10^3	1126.7	3.6	2295.5	6.8	3033.6	1.60
2.0	15.7	595.2	$2.5 \cdot 10^5$	1358.5	2.3	3318.9	10.5	3817.2	1.50
3.0	14.3	486.2	–	1478.6	1.9	4087.7	15.0	4238.2	1.45
5.0	13.6	349.8	–	1565.0	1.7	4593.4	19.5	4533.2	1.42
10.0	13.1	159.1	–	1639.1	1.6	4983.8	21.8	4775.8	1.39
20.0	12.9	203.8	–	1678.2	1.5	5150.4	20.4	4893.1	1.37
30.0	12.84	229.3	–	1687.3	1.5	5192.3	19.8	4918.2	1.36
40.0	12.81	237.2	–	1689.7	1.5	5211.5	20.0	4925.5	1.36
50.0	12.78	242.2	–	1693.2	1.5	5228.5	19.9	4936.4	1.36

Table 2. The same as in Table 1 but for model B. The main difference between the two models is that model A does not have a phase transition to quark matter in the inner core, while model B develops a quark core at about $t = 20$ s. The initial and final gravitational mass are the same as for model A.

t	R	ν_{g_1}	τ_{g_1}	ν_f	τ_f	ν_{p_1}	τ_{p_1}	ν_{w_1}	$10^4 \times \tau_{w_1}$
0.20	35.1	582.5	24.5	942.2	69.2	1145.1	14.2	1489.9	2.06
0.25	32.2	636.0	19.5	939.0	43.2	1279.0	11.3	1653.7	1.98
0.30	30.0	682.0	16.6	934.2	32.5	1392.2	9.7	1796.3	1.93
0.40	27.1	750.0	14.8	926.2	19.0	1573.4	8.3	2028.0	1.84
0.50	25.1	790.0	18.6	927.0	10.9	1718.0	7.9	2208.9	1.79
0.60	23.6	805.3	35.2	941.4	7.2	1843.2	7.8	2357.0	1.75
0.70	22.6	803.4	75.2	962.6	5.8	1942.8	7.9	2471.5	1.72
0.75	22.2	799.0	108.0	974.0	5.4	1985.0	8.0	2520.9	1.71
1.0	20.5	767.0	593.0	1033.0	4.4	2181.0	8.6	2743.5	1.66
2.0	17.0	640.0	$5 \cdot 10^4$	1213.0	2.9	3036.0	13.5	3369.3	1.56
3.0	15.3	533.0	–	1316.0	2.4	3807.0	21.0	3742.9	1.52
5.0	14.4	374.0	–	1405.0	2.1	4437.0	32.7	4050.1	1.48
10.0	13.9	168.0	–	1475.5	2.0	4951.8	43.0	4285.2	1.44
20.0	13.7	232.6	–	1501.5	1.9	5144.8	42.9	4364.6	1.42
30.0	13.5	257.4	–	1547.1	1.8	5174.5	28.2	4486.6	1.40
40.0	13.3	476.2	–	1603.9	1.7	5231.2	18.1	4640.6	1.39
50.0	13.2	489.0	–	1606.9	1.7	5251.5	17.9	4649.4	1.38

Table 3. The initial amplitude h_0 that a gravitational signal emitted by a PNS oscillating in the various modes should have, at the detector site, to be detectable by the VIRGO I, LIGO I, GEO600 and EURO interferometers, with a SNR= 5. We also show the corresponding energy E_{GW} (in units of $M_\odot c^2$) emitted in GWs for each mode, if the source is located at a distance of $D = 10$ kpc. Notice that the energy scales as D^2, and the required energy to detect the same signal at the Virgo cluster (15 Mpc) is $2.25 \times 10^6 E_{GW}$.

QNM		VIRGO I	LIGO I	GEO600	EURO
g_1–mode	h_0	3.6×10^{-22}	8.3×10^{-22}	2.0×10^{-21}	1.4×10^{-24}
	E_{GW}	8.2×10^{-9}	4.3×10^{-8}	2.5×10^{-7}	1.2×10^{-13}
f–mode	h_0	2.3×10^{-22}	6.2×10^{-22}	1.6×10^{-21}	8.2×10^{-25}
	E_{GW}	3.5×10^{-8}	2.7×10^{-7}	1.7×10^{-6}	4.6×10^{-13}
p_1–mode	h_0	3.8×10^{-22}	1.2×10^{-21}	3.1×10^{-21}	1.3×10^{-24}
	E_{GW}	7.2×10^{-7}	6.5×10^{-6}	4.7×10^{-5}	8.2×10^{-12}
w_1–mode	h_0	2.8×10^{-20}	4.6×10^{-20}	9.3×10^{-20}	1.1×10^{-22}
	E_{GW}	5.9×10^{-8}	1.6×10^{-7}	6.1×10^{-7}	9.5×10^{-13}

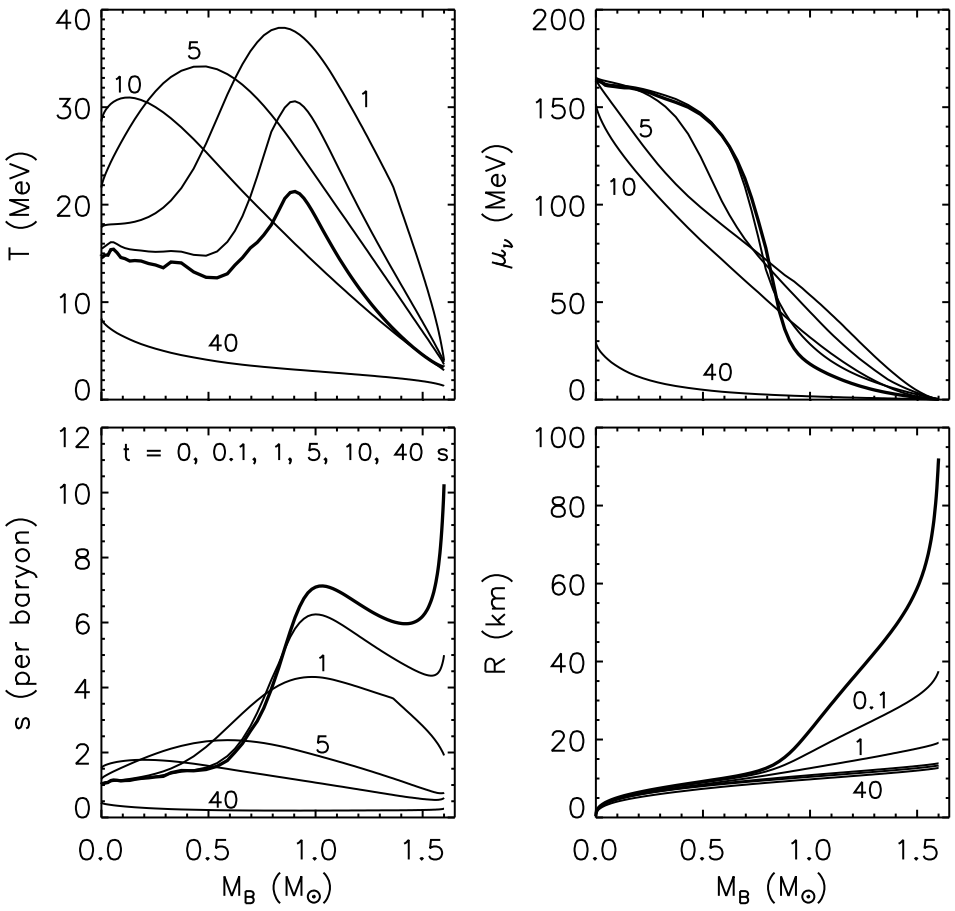

Figure 1. Temporal evolution of the temperature T, entropy per baryon s, neutrino chemical potential μ_ν, and radius R, as a function of the enclosed baryonic masses M_B for model A. The thick line is the initial profile and the figure displays a temporal sequence corresponding to $t = 0.1, 1, 5, 10$ and 40 seconds of evolution.

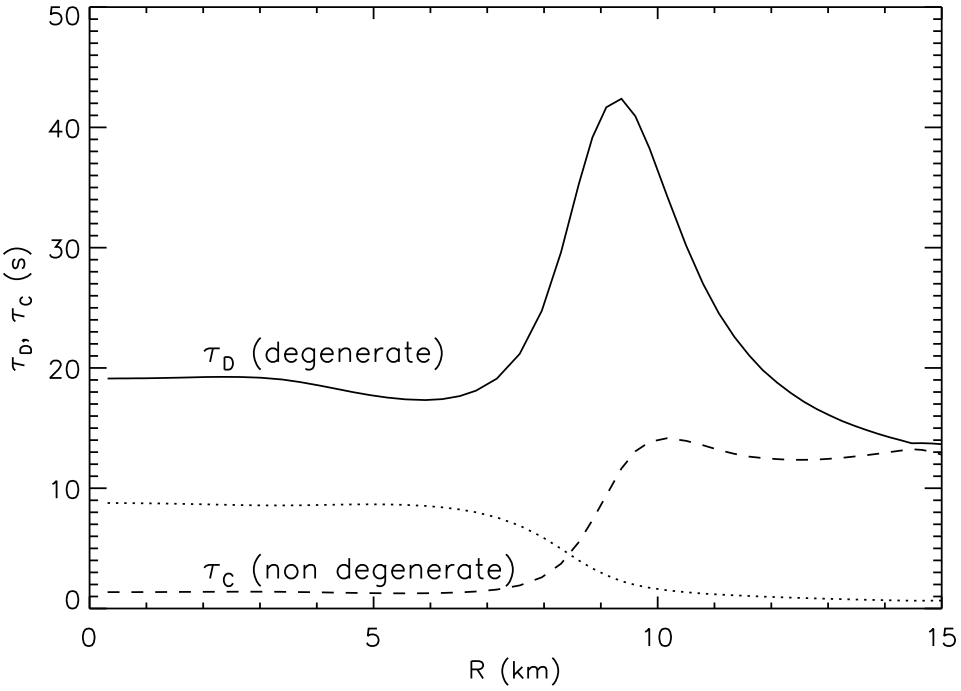

Figure 2. Neutrino dissipation timescales corresponding to diffusion (τ_D) and thermal conductivity (τ_C) at $t = 0.25$ s for model A in the inner 15 km of the PNS. The diffusion timescale (solid line) dominates in the degenerate regime, while the conductive timescale (dashes) applies to matter with non–degenerate neutrinos. For reference, we also show the dimensionless neutrino degeneracy parameter, $\eta = \mu_\nu/T$ (dotted line), which indicates that the regime is degenerate from the star center up to about 10 km, while it is non degenerate in the outer, low density, region.

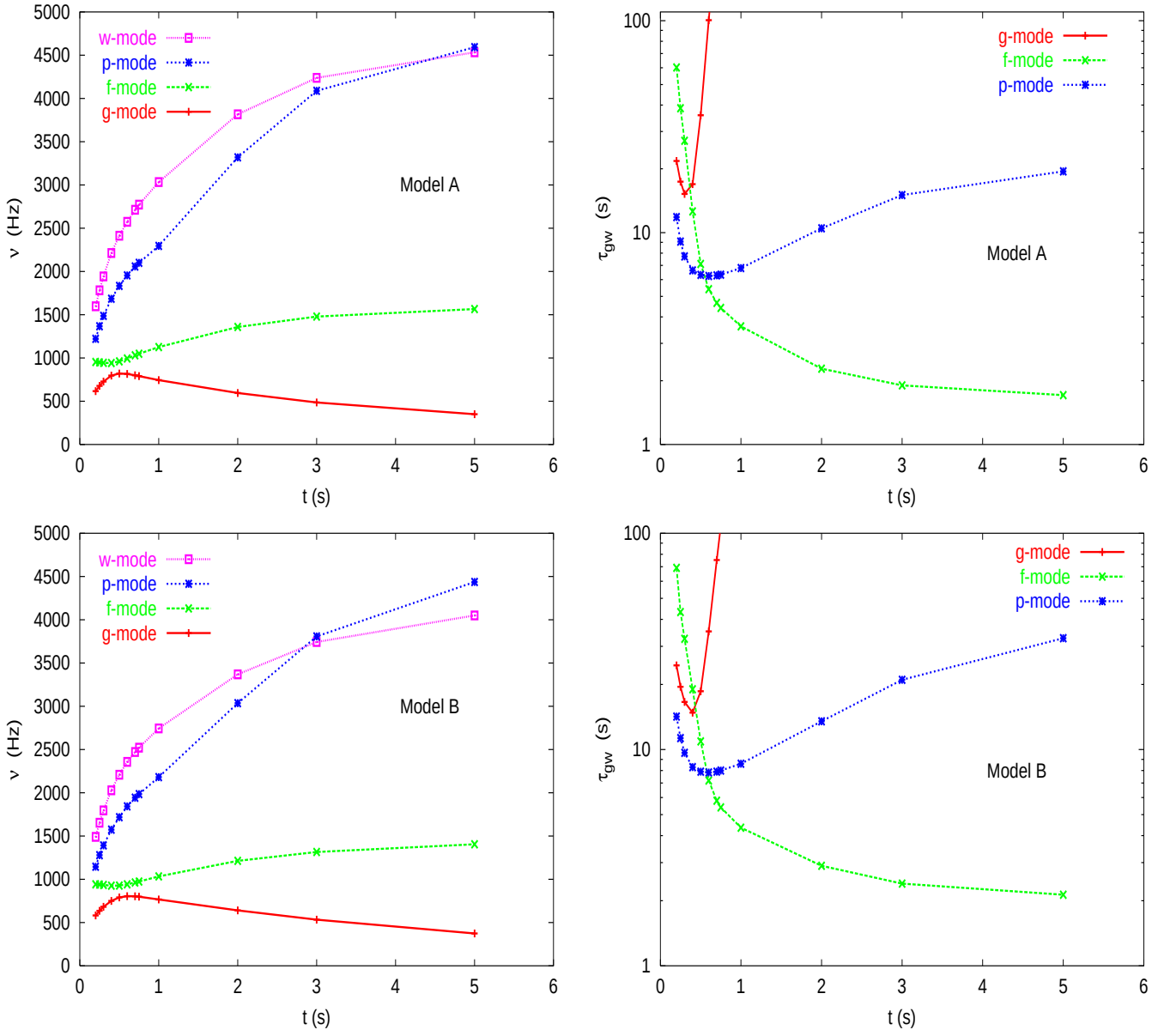

Figure 3. The frequencies and damping times of the lowest QNMs of the proto–neutron star are plotted as a function of the time elapsed from the gravitational collapse, during the first 5 seconds of evolution. The data plotted in the upper panel refer to model A (see Table 1) while the lower panel refers to model B (see Table 2), whose main difference from model A is the appearance of a quark core at some instant of the evolution. Note that the overall behavior is the same for both models, the frequency of all the modes clusters in a very narrow range at the beginning of the PNS evolution and begins to differentiate after less than 1 second. After a few seconds the behavior is already well established and the QNM frequencies tend to their values for old, cold NSs. Note also that the g–mode damping time reaches a deep minimum at about $t = 0.3$ s. The gravitational damping time of the w–mode is not shown because it is too small with respect to the scale of the figure, $\tau_w = [1.4 - 2.1] \cdot 10^{-4}$ s.

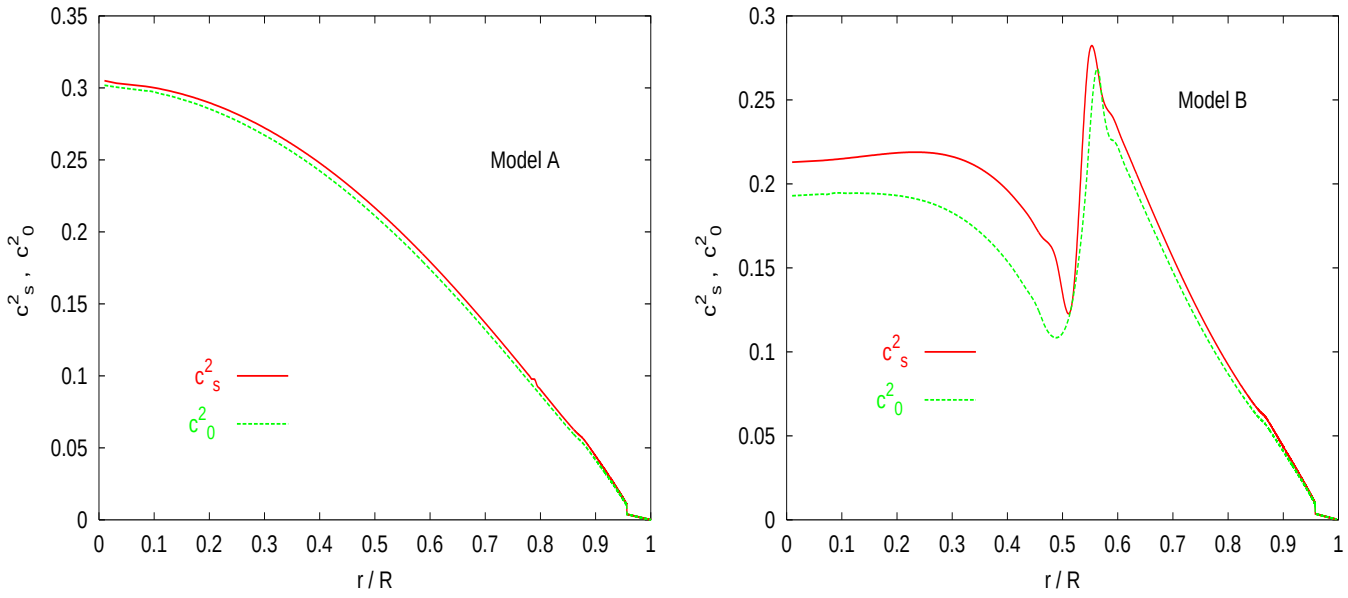

Figure 4. The square of the sound velocity c_s and of the equilibrium velocity c_0 (see Section 3) for model A and B, as a function of the radial coordinate at $t = 50$ s. The difference between the two stellar models is due to the presence of a quark matter core in model B for $r < 0.54R$. The larger difference between c_s^2 and c_0^2 in the quark core explains the higher value of ν_{g_1} for model B at the end of the evolution.

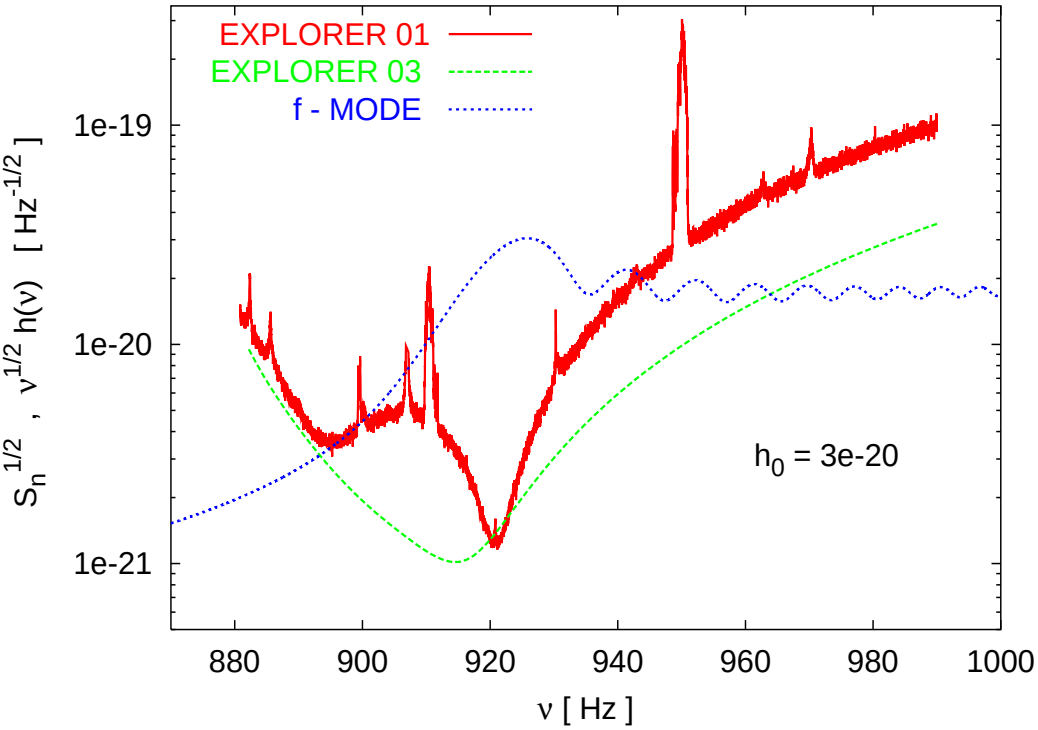

Figure 5. The strain amplitude of the gravitational signal produced by a proto–neutron star oscillating in the f–mode is plotted as a function of the frequency. The signal is assumed to have an initial amplitude of $h_0 = 3 \times 10^{-20}$ (see Section 4). In the same figure we also plot the experimental noise strain amplitude of the resonant detector EXPLORER obtained in December 2001, and the strain noise curve that the EXPLORER team expect to obtain in 2003.

REFERENCES

Andersson N., Kokkotas K.D., 1996, Phys. Rev. Lett., 77, 4134

Andersson N., Kokkotas K.D., 1998, MNRAS, 299, 1059

Astone P., 2002, Class. Quant. Grav. , 19,7

Benhar, O., Berti, E. and Ferrari, V., 1999, MNRAS, 310, 797

Brown, J.D., 2001, in AIP Conference Proc., 575, 234

Burrows A., Lattimer J. M., 1986, ApJ, 307, 178

Chandrasekhar S., Ferrari V., 1991, Proc. R. Soc. London A, 432, 247

Detweiler S., Lindblom I., 1985, ApJ, 292, 12

Dimmelmeier H., Font J.A., Müller E., 2002, A&A, 393, 523

Finn L.S., 1987, MNRAS, 227, 265

Freyer C.L., Holz D.E., Hughes, S.A., 2002, ApJ, 565, 430

Glendenning N.K., Moszkowski S., 1991, Phys. Rev. Lett., 67, 2414

Goodwin B.T., Pethick C.J., 1982, ApJ, 253, 816

Grishchuk L.P., Lipunov V.M., Postnov K.A., Prokhorov M.E., Sathyaprakash B.E., 2001, Physics Uspekhi, 44, 1

Kokkotas K.D., Schutz, B.F., 1992, MNRAS, 255, 119

Lai D., 1994, MNRAS, 270, 611

Leins M., Nollert H.-P., Soffel M.H., 1993, Phys. Rev., D 48, 3467

McDermott P.N., van Horn H.M., Hansen C.J., 1988, ApJ, 325, 725

Miniutti G., Pons J.A., Berti E., Gualtieri L., Ferrari V., 2003, MNRAS, 338, 389

Müller H., Serot B.D., 1996, Nucl. Phys., A 606, 508

Pons J.A., Reddy S., Prakash M., Lattimer J.M., Miralles J.A., 1999, ApJ, 513, 780

Pons J.A., Miralles J.A., Prakash M., Lattimer J.M., 2000, ApJ, 553, 382

Pons J.A., Steiner A.W., Prakash M., Lattimer J.M., 2001, Phys. Rev. Lett., 86, 5223

Prakash M., Bombaci I., Prakash M., Ellis P.J., Lattimer J.M., Knoren R., 1997, Phys. Rep. 280, 1

Rampp, M., Müller, E., Ruffert, M., 1998, A&A, 332, 969

Reisenegger A., Goldreich P., 1992, ApJ, 395, 240

Shibata M., Uryu K., 2000, Phys Rev D61, 064001

Shibata M., Uryu K., 2002, Prog.Theor.Phys., 107, 265

Sotani H., Tominaga K., Maeda K., 2002, Phys. Rev., D 65, 024010

Strohmayer T.E., 1993, ApJ, 417, 273

Thorne K.S., 1966, ApJ, 144, 201

van den Horn L.J., van Weert C.G., 1984, A&A, 136, 74

Zerilli J.F., 1970, Phys. Rev., D 2, 2141

Zwerger T., Müller E., 1997, A&A, 320, 209